Solar Energy 155 (2017) 167–177

Contents lists available at ScienceDirect

Solar Energy

journal homepage: www.elsevier.com/locate/solener

Performance prediction of chalcopyrite-based dual-junction tandem solar cells

Kihwan Kim, Jin Su Yoo, Seoung Kyu Ahn, Young-Joo Eo, Jun-Sik Cho, Jihye Gwak, Jae Ho Yun *

Photovoltaic Laboratory, Korea Institute of Energy Research, Daejeon 34129, Republic of Korea

ARTICLE INFO

Article history:
Received 17 March 2017
Received in revised form 22 May 2017
Accepted 26 May 2017

Keywords:
CIGS
Tandem
Multi-junction
Simulation

ABSTRACT

In this work, we present SCAPS-1D simulations of $Cu(In,Ga)Se_2$-based dual-junction tandem cells. The purpose of this work is to assess the device performances of the $Cu(In,Ga)Se_2$-based tandem cells based on the fact that each subcell is simulated to yield a reported best efficiency at its bandgap. A method to build the J-V characteristics of tandem cells from individual J-V curves of subcells is also discussed. By thinning the absorber thickness of the top subcell, the current matching points among various bandgap combinations are examined. In spite of neither optical nor electrical loss between the top and bottom subcells, the device performances of the tandem devices do not substantially surpass the device performances of single-junction devices, which is ascribable to the relatively poor efficiencies of the wide-bandgap top subcells. We also discuss how further improvements in the wide-bandgap top subcells are needed to create a validity for making an effortful multi-junction device.

1. Introduction

One way to overcome efficiency from a typical solar cell is to make a multi-junction tandem solar cell by stacking the junctions serially. In theory, infinite stacking of junctions can yield an efficiency of 65.4% under AM 1.5 illumination, and even further improvement in performance (i.e., 85%) can be achieved with a concentrated incident spectrum (Martí and Araújo, 1996). Typically, III–V and a-Si solar cells are fabricated with a tandem device structure for an efficiency enhancement, and indeed, 46%- and 13.6%-efficient cells have been demonstrated, which surpasses the efficiency of a single-junction solar cell (Green et al., 2016).

In tandem solar cells, two or more subcells are serially connected and should properly share the incident spectrum. In other words, the top subcell should partially absorb the incident solar spectrum and let the unabsorbed spectrum pass through to the bottom subcells. This requirement brings multiple obstacles and restrictions for making a tandem solar cell. First, subcells are connected with a transparent tunnel junction so that charge carriers and unabsorbed photons can pass through the tunnel junction with minimized loss. Second, excepting the very bottom subcell, the top subcells should be properly thinned to achieve a current matching condition among the subcells. In principle, the tandem solar cells are "electrically" considered as a serially connected solar cell, and as a result, the subcell with the lowest current density (assume that all the subcells have an identical device area) naturally becomes the current limiting device in the connection. Therefore, by matching the current density similarly (ideally, matched identically) among subcells, the most efficient operation of the tandem solar cells can be guaranteed. Third, the fabrication of multi-junction solar cells typically involves high temperature processes. In particular, the high temperature process during the top subcell fabrication should result in a thermal stress to the pre-existing subcells unless the subcells are mechanically stacked. In particular, unintended inter-diffusion or excess diffusion typically occurs in the bottom subcells and therefore the resulting tandem solar cell does not works as designed (Shafarman and Paulson, 2005; Nishiwaki et al., 2003; Nakada et al., 2006).

Up to now, $Cu(In,Ga)Se_2$ (CIGS)-based solar cells have shown impressive progress in the film-film photovoltaic (Jackson et al., 2016; Reinhard et al., 2015; Nakamura et al., 2015). This absorber material and its variations (e.g., Ag or S alloying) are bandgap (E_g)-tunable and thus potentially allow their extension to a tandem solar cell (Avon et al., 1984; Kim et al., 2016; Kim et al., 2015; Bär et al., 2004; Hanket et al., 2009). Obviously, numerous studies have attempted to demonstrate CIGS-based tandem solar cells (Shafarman and Paulson, 2005; Nakada et al., 2006; Young et al., 2002; Jehad et al., 2005); however, leaving an improved efficiency aside, even a similar efficiency has not been reported compared with a single-junction device. Fundamentally, the achieved efficiencies from wide bandgap CIGS-based solar cells (i.e., $Eg \geq 1.4$ eV) do not seem to be sufficient for accomplishing any improvement in the device performance by using the tandem struc-

* Corresponding author.
E-mail address: yunjh92@kier.re.kr (J.H. Yun).

http://dx.doi.org/10.1016/j.solener.2017.05.080
0038-092X/

ture (Contreras et al., 2011; Kim et al., 2017); nevertheless, in reality, several technical issues continue to impede even the viable operation of the CIGS-based tandem solar cells. To the best of our knowledge, only an efficiency of 2.7% has been obtained from a CIGS-based monolithic tandem cell since the early 2000 s (Shafarman and Paulson, 2005). Most of all, the absence of suitable tunnel junctions and relatively poor thermal stability of the bottom CIGS-based subcell have been considered as major technical barriers (Kijima and Nakada, 2008). Instead, mechanically stacked CIGS tandem cells (Nishiwaki et al., 2003; Nakada et al., 2006; Young et al., 2002) or hybrid multi-junction cells (e.g. Perovskite/CIGS and Dye-sensitized cell/CIGS) (Bailie et al., 2015; Liska et al., 2006) have also been extensively studied because this approach offers a relatively wide process window for the cell stacking. Nevertheless, obtained efficiencies from the alternative approaches do not overcome an efficiency from an optimized single junction CIGS cell.

The various advantages of CIGS as a photovoltaic material have inspired various efforts for making CIGS-based or CIGS-including tandem cells (Bailie et al., 2015; Shafarman et al., 2010; Wenger et al., 2009; Kranz et al., 2015). Depending on where and/or how the CIGS-based solar cells were placed (i.e., top vs. bottom vs. top and bottom), narrow (typically 1.0 eV)- or wide (typically 1.6–1.7 eV)-bandgap CIGS solar cells have been chosen. Based on the fact that the CIGS solar cells exhibit a strong correlation between bandgap and efficiency (Shafarman et al., 1996), various combinations of top and bottom subcells should be examined carefully to ensure the highest efficiency from the tandem structure.

In this work, with the SCAPS-1D simulation package, potential efficiencies of CIGS-based dual-junction tandem solar cells are examined. Firstly, CIGS solar cells with a single junction were simulated to exhibit state-of-the-art efficiencies in various bandgaps ranging from 1.0 to 1.7 eV with an interval of 0.1 eV. The CIGS solar cells with Eg = 1.5 to 1.7 eV (interval = 0.1 eV) were chosen as the top subcell in the tandem solar cell, while the cells with Eg = 1.0 to 1.2 eV (interval = 0.1 eV) were placed as the bottom subcell. As discussed above, two subcells in the tandem cells are connected serially, and there should therefore be a proper current density for ensuring efficient operation of the tandem cell. In the present study, two types of current matching points were examined: (1) matching J_{SC} (short-circuit current density) and (2) matching J_{MP} (current density at the maximum power point). The current matching points (by the two methods) were obtained by thinning the top subcell's absorber thickness. Then, the device performances of the top subcells and the transmitted light spectra through the top subcells were simulated by thinning their absorber thicknesses. The transmitted light spectra were used as the incident light spectra for the bottom subcells' simulations. Because J-V curves of top- and bottom-subcells were obtained separately, two J-V curves should be merged to build J-V curves of tandem cells. We also investigated how to construct J-V curves from the individual J-V curves of each subcell by measuring the J-V characteristics of serially connected cells. The obtained results suggested that any combination in the present work showed that the device performance of the tandem cell is similar to the highest efficiency from single-junction devices (Jackson et al., 2016; Jackson et al., 2015; Chirilă et al., 2013), indicating that the top-subcells' performances significantly limit the resulting performance of the tandem cell. Finally, we also discussed how further device improvement is required to achieve a substantially higher efficiency from a tandem device compared with a single-junction device.

2. Methods

Simulated dual-junction tandem solar cells were designed using the structure shown in Fig. 1. It is assumed that the CIGS-based tandem solar cells have an ideal tunnel junction, having neither electrical resistance nor optical loss, between the top and bottom subcells. The current matching conditions were examined by changing the thickness of the absorber in the top subcell. It is also assumed that the optical loss and interference in each interface are negligible. The SCAPS-1D simulation tool does not fully support a solar cell with a multi-junction structure, and therefore, by simulating top and bottom subcells separately, the current matching conditions were found.

First, based on the NUMOS model (i.e., one of the default models in the SCAPS-1D simulation package), single-junction CIGS solar cells with various bandgaps (Eg = 1.0 to 1.7 eV, interval = 0.1 eV) were simulated (Burgelman et al., 2007; Degrave et al., 2003; Burgelman et al., 2000); the absorption coefficients of the CIGS absorber layers were interpolated from P. D. Paulson's work (Paulson et al., 2003). The measured absorption data of Ref. (Paulson et al., 2003), however, exhibit non-zero values in the sub-bandgap range, thus resulting in unrealistic charge collections in the sub-bandgap range. Therefore, the absorption coefficients corresponding to the sub-bandgap range were also modified.

Table 1 lists the basic input values for the single-junction CIGS cells' simulations. It was assumed that the wide bandgap CIGS solar cells (Eg = 1.5, 1.6, and 1.7 eV), used as the top subcell in the tandem solar cell, do not have an internal bandgap gradient. As will be discussed later, the absorber thinning process of the top subcell is indispensable in tandem solar cells, so the internal bandgap gradient in the absorber bulk significantly increases the complexity of the simulation. When used as the bottom subcells, however, narrow bandgap CIGS solar cells ($Eg \leq 1.2$ eV) were assumed to have bandgap gradients in the absorber bulk (except the case of $E_g = 1.0$ eV, pure CIS). Most of the highly efficient devices exhibit a compositional gradient (consequently, bandgap gradients) inside their absorber bulks (Jackson et al., 2015; Chirilă et al., 2011). Thus, to best simulate CIGS solar cells, the bandgap gradients should be introduced. The bandgap profiles of the CIGS absorbers ($E_g = 1.1$ and 1.2 eV) are also available in supplementary information.

The method for finding the current matching point between the two subcells is straightforward. With the thinning of the top cells' absorber layer from 2.0 to 0.2 μm, the J_{MP} and J_{SC} of the top CIGS subcell along with the transmitted spectra were calculated. The reason for limiting the top subcell's thickness to 0.2 μm is practically difficult to achieve viable device properties in such a thin absorber. The transmitted spectrum, S(λ), is given by:

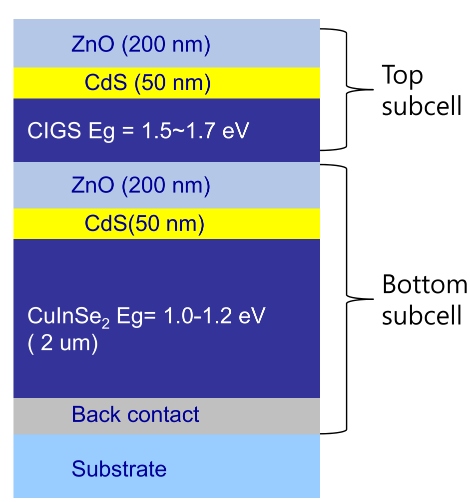

Fig. 1. Schematic drawing of a simulated dual-junction solar cell.